Int J Mater Form (2017) 10:697–705
DOI 10.1007/s12289-016-1312-9

ORIGINAL RESEARCH

High strain rate embossing with copper plate

Huimin Wang[1] · **Anupam Vivek**[1] · **Yuliang Wang**[2] · **Gopal Viswanathan**[1] · **Glenn Daehn**[1]

Received: 29 October 2015 / Accepted: 5 August 2016 / Published online: 11 August 2016

Abstract Embossed parts, that contain a number of features, are desired for a range of components, such as, heat exchangers, bipolar plates, micro-reactors, and micro-fluidics. A comparison of low strain rate embossing and high strain rate embossing was investigated in this study. High strain rate deformation at the embossed surface induced quatitatively different properties than those on a quasi-statically formed part. A commercial hand file was chosen as a simple and available die surface due to its high hardness and relatively fine features. Commercially pure copper (110) was embossed using four methods: quasi-static (static, low strain rate), magnetic pulse (MP, high strain rate), direct vaporizing foil actuator (direct VFA, high strain rate), and urethane-assisted vaporizing foil actuator (urethane VFA, high strain rate). Embossed depth, mechanical properties, and microstructure evolution were studied for both low strain rate embossing and high strain rate embossing. The results showed that generally better conformity to the die features and higher surface hardness were achieved with high strain rate embossing, in part because higher pressures could be developed with these methods. The study of the microstructure revealed that besides the grain size and shape change, significant twinning appeared along the deformed surface in high strain rate embossed parts. Optical microscopy (OM), scanning electron microscopy (SEM), and transmission electron microscopy (TEM) were performed to study the resultant microstructure.

Keywords High strain rate embossing · Magnetic pulse (MP) · Vaporizing foil actuator (VFA) · Micro-hardness · Twinning

✉ Huimin Wang
wang.1333@osu.edu

✉ Glenn Daehn
daehn.1@osu.edu

[1] Department of Materials Science and Engineering, The Ohio State University, 2041 College Rd, Columbus, OH 43210, USA

[2] Robotics Institute, School of Mechanical Engineering and Automation, Beihang University, Beijing 100191, People's Republic of China

Introduction

Components with varied micro features have been widely used in many fields [1], such as automotive [2], medical devices [3], electronics [4]. The pressures needed for traditional mechanical forming of such features are generally about 3 times higher than the flow stress of the material [5]. Therefore, large size component fabrication is very difficult due to the significantly high load requirements from the press, and even small components can be difficult to form due to high stresses on the tool. Besides the load requirements, there is also an issue of decreased formability when the features to be formed are on the same scale as the grain size. Such effect was shown by Gau et al. for tensile formability of aluminum and brass [6]. One method used to reduce the flow stress of workpiece is electrically-assisted embossing [3]. In this method, high density current is passed through the workpiece and the die during the embossing process. As the die and the workpiece come together, the current passes through the contact area, thereby causing local Joule heating. Due to the Joule heat and some investigators believe there may be an important electroplasticity effect [7–9], whereby the flow stress of the workpiece is reduced due to the current density in addition to the Joule heating.

Embossing at high strain rate can be advantageous in several ways. First, a modest pressure can be used to accelerate a workpiece over a distance and deceleration on impact can

produce a much higher pressure than the driving pressure used for launching the workpiece. Equation 1 [10] can be used for calculating the impact pressure in an elastic collision, where ρ_1 and ρ_2 are densities of workpiece and the die, C_1 and C_2 are sound velocities of workpiece and die, V_i is the impact velocity. For a copper sheet impacting a steel die at 150 m/s the impact pressure can be estimated to be 3.4 GPa. Second, if the forming is implemented through passage of a high pressure impulse or shock wave through the workpiece, shock hardening can produce finer microstructures and higher hardness. Third, as a single die is used, the system is simple and can have high dimensional tolerance. Impulse based forming has also been demonstrated to result in reduced springback, which causes better die conformity [11].

$$P_i = \frac{\rho_1 \rho_2 C_1 C_2}{\rho_1 C_1 + \rho_2 C_2} V_i \tag{1}$$

Microstructural evolution of materials deformed at high strain rate has been studied widely. The increase in strength of copper with high strain rate deformation was studied in detail by Meyers et al. [12]. High density twins were observed in the sample. Since then, deformation twins in deformed copper have been observed by several other researchers [13–16]. In those studies, methods such as explosive-driven, electro-discharge, and impact anvil were used to generate sharp high pressure. An optimization study of surface hardening by ball impact on stainless steel 304 was conducted by Chan et al. [17]. They found out that higher strain rate promoted more desirable nanostructure with increased number of nano-twins, which was considered as the main reason for the exceptional mechanical properties obtained by them. To fabricate the nanostructural alloys, it is known that high strain rate has equivalent effect with low temperature. The combination effect is known as Zener-Hollomon parameter (defined as Z). In low Z process, dislocation activities dominate the grain refinement. In high Z process, deformation twinning is the dominate microstructure. The number of twins increases with higher Z [18]. Cryogenic rolling is one of the low temperature methods to induce the nanostructural alloys, which promotes enhanced strength and higher hardness [19].

In this paper, quasi-static (static), magnetic pulse (MP) [20], direct vaporizing foil actuator (direct VFA) [21], and urethane-assisted vaporizing foil actuator (urethane VFA) forming [21] were used to drive a commercially pure copper alloy against a simple die, a file surface. Among those four, MP, direct VFA, and urethane VFA are high strain rate forming methods. The relationship between the depth of the grooves on embossed copper and the experimental parameters such as input energy and driving pressure was established. Variations in material microstructure and mechanical properties that result from both the low strain rate and high strain rate forming processes are also discussed in this paper.

Experimental procedure

Die and workpiece

A commercial hand file was chosen as the die, which is generally made of plain carbon tool steel. It is a rectangular single-cut tapered edge hand file obtained from McMaster-Carr (Part number: 4225A36). As obtained, the file was 356 mm long, 33 mm wide, and 6 mm thick. It was cut to requisite sizes for the different types of experiments. Figure 1 illustrates the surface of the die at different magnifications. The third image is a 3D representation of the surface obtained through splicing together of images taken at different focal depths by the Keyence digital microscope. From that, the groove of the file was found to be 350 μm deep and 580 μm wide. The dimensions of the die in static and high strain rate experiments were 25 mm × 15 mm and 100 mm × 33 mm, respectively. In the static experiment, the size of the die was selected based on the estimated pressure and capacity of the hydraulic press. In the MP experiment, the length of the die was limited by the size of the uniform pressure actuator (UPA) [20]. In the direct/urethane VFA experiment, the length of the die was selected based on the selection for the dimension of the foil actuator.

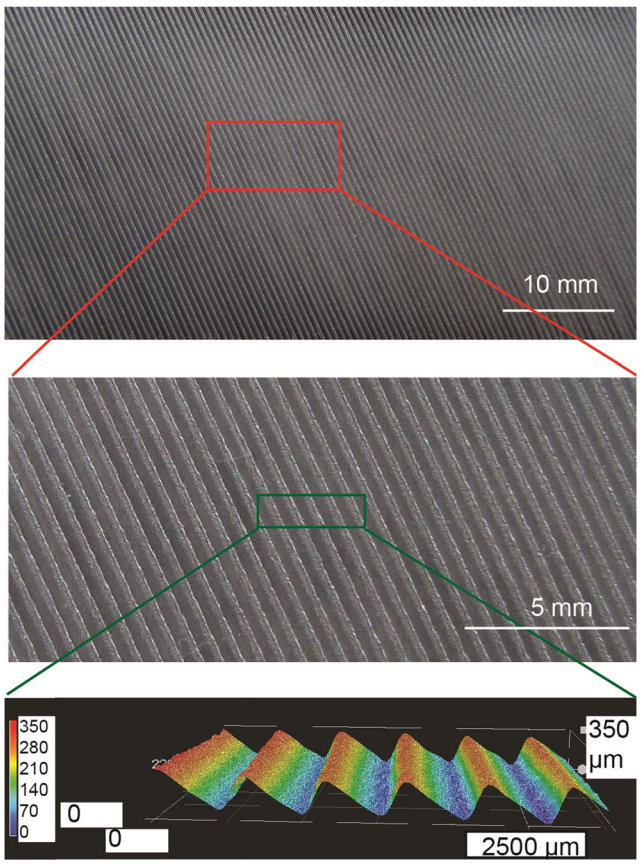

Fig. 1 Commercial standard single fine cut file surface from low to high magnification. The third image is 3D surface of the file measured by Keyence digital microscope. The color represents the height of the surface

Annealed copper alloy 110 sheet, which was 254 μm thick, was used as the workpiece. The grain structure of the original Cu110, shown in Fig. 2, reveals equiaxed grains with an average grain size of nearly 15 μm. For every formed workpiece, the groove depth was measured using optical microscope with mounted samples. Micro-hardness was measured using a 25 g load and a dwell time of 20 s with automated micro-hardness test machine.

Quasi-static (static) experimental setup

The static experiment was done on a standard MTS hydraulic press. A schematic representation of the experimental setup is given in Fig. 3a. The force, which was applied at the rate of 1–2 kN/s, was transferred from the press to the workpiece via layers of steel and cardboard. The static experiment was carried out under pressure of 50 MPa, 100 MPa, 150 MPa, 200 MPa, 250 MPa, 300 MPa, 400 MPa, 600 MPa, 800 MPa.

Magnetic pulse (MP) experimental setup

MP or electromagnetic pulse forming is a high strain rate forming method, which relies on the discharge process of capacitors to generate magnetic pressure. In this study, the capacitor bank [22] energy can be adjusted between 0 and 16 kJ. For MP method, UPA (shown in Fig. 3c), was used to launch the workpiece. The coils for the UPA [20] used in these experiments were made out of a high strength copper alloy. It consisted of an inner solenoid coil with 12 turns and a single turn outer channel. The gap between the solenoid coil and the outer coil was filled with a cured polyurethane. In this experiment, the solenoid coil was connected with the terminals of the capacitor bank [23] to form the primary electrical circuit. The workpiece contacted with the outer coil to form the secondary electrical circuit, as shown in Fig. 3b. When the capacitor bank was discharged, the transient current passing through the inner coil induced eddy currents in the workpiece. Due to the electromagnetic interaction between the solenoid coil and the workpiece, which carried currents in opposite directions, repulsive forces were generated between them. As a result, the workpiece was launched at varying speeds into the die. Input energy levels of 2.4 kJ, 3.2 kJ, 4.0 kJ, 4.8 kJ, 5.6 kJ, 6.4 kJ were selected. The workpiece velocity was measured using Photonic Doppler Velocimetry (PDV) system [24]. The standoff distance between the die and the workpiece is 2 mm. The choice of this distance was based on the optimization to have maximum velocity.

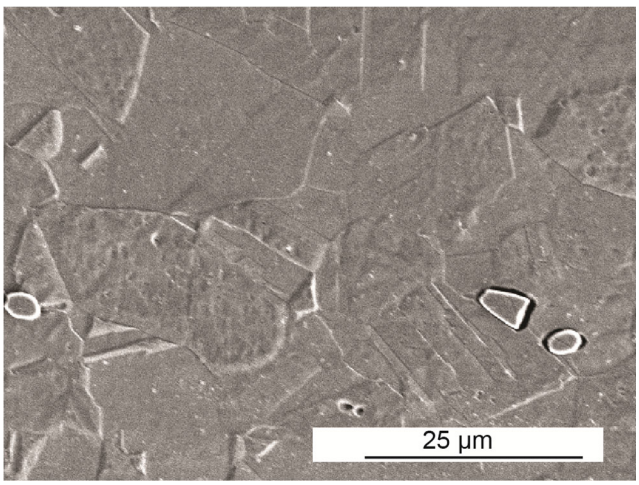

Fig. 2 Microstructure of as-received Cu110 shows equiaxed grains with an average grain size of about 15 μm

Direct vaporizing foil/urethane-assisted vaporizing foil (direct/urethane VFA) experimental setup

The experimental setup for vaporizing foil method is shown in Fig. 3d and e. The ends of a 75 μm thick aluminum foil shaped in the form of a dog-bone were connected to the terminals of the capacitor bank. The passage of a capacitor bank driven current through the foil led to its rapid vaporization which created the pressure to drive the workpiece placed directly above it. The narrow part of the foil, which bursts first and is considered as the active region, was 15 mm wide and 100 mm long. The foil actuator was insulated from the workpiece and the base plate by using a polyimide tape. There were two configurations in which vaporizing foil was used to drive the workpiece: (i) workpiece placed directly against the insulated foil actuator, named as direct VFA, (ii) a pressure transfer medium in the form of a urethane pad placed between the foil actuator and the workpiece. For the second configuration, the rapid vaporization of the foil shock loads the elastomer medium. The high-pressure pulse propagates through the medium and launches the workpiece into the die. The medium also helps in uniformly distributing the pressure over a larger area. In this study, a urethane pad (80 A) with dimensions of 100 mm × 76 mm × 12.5 mm was selected. Therefore, this method is named urethane VFA. Besides the consideration of pressure, it is expected that the urethane pad would thermally isolate the workpiece from the hot gases resulting from the foil vaporization. The heat effect from the plasma would be negligible. For direct VFA forming, the capacitor bank energy levels at 1.6 kJ, 2.4 kJ, 3.2 kJ, 4.0 kJ, and 4.8 kJ were selected until to have fully deformed workpiece. For urethane VFA forming, input energies of 8.0 kJ and 9.6 kJ were selected based on previous experimental experience not to damage the urethane pad. From the energy efficiency standpoint, urethane VFA should have lower energy efficiency than direct VFA due to the energy loss within the urethane pad. Therefore, a larger input energy was used for urethane VFA forming. The dimension of the central part of the foil determines the size of the deformed copper. For the direct VFA, the deformed copper had a similar dimension to the central part of

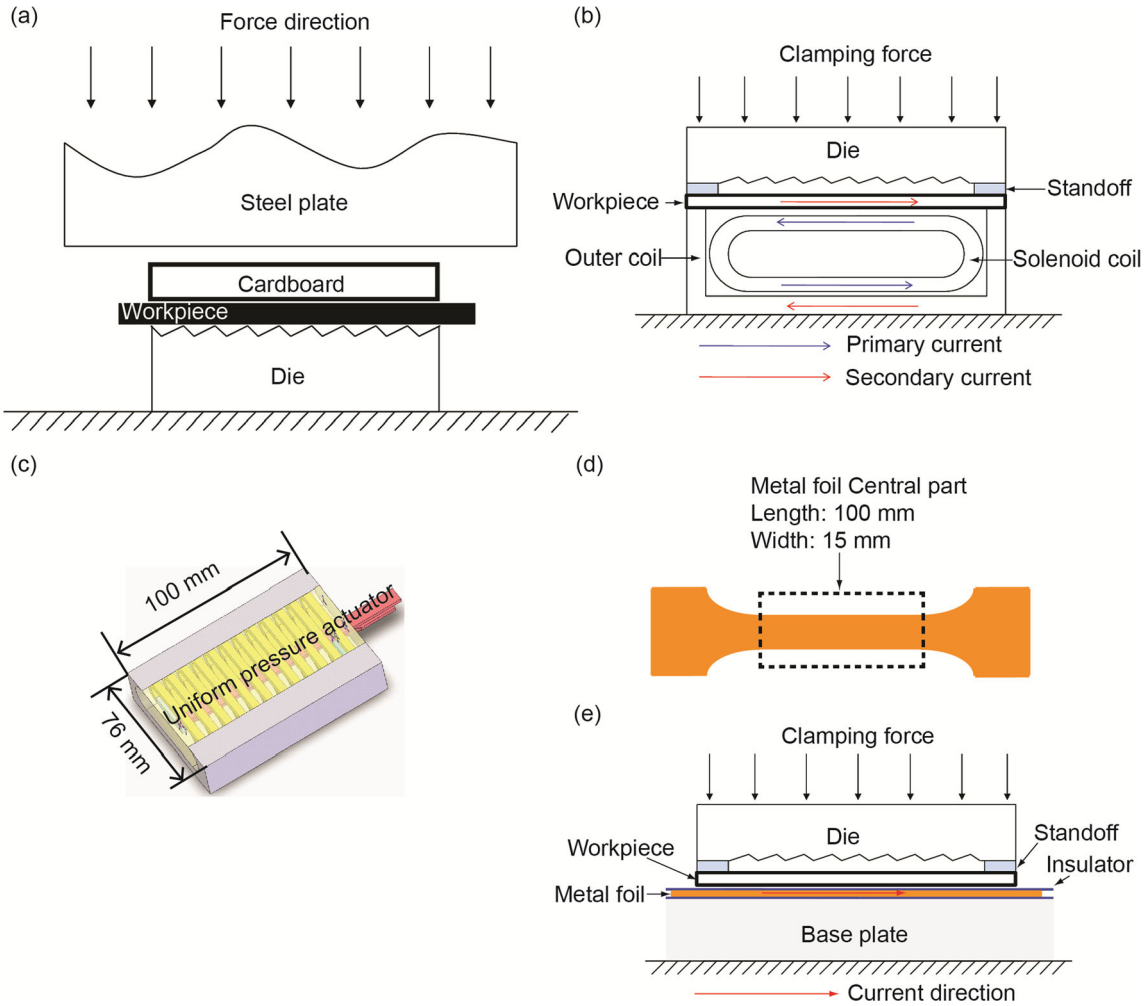

Fig. 3 **a** Schematic static experimental setup. The pressure is controlled by the standard MTS hydraulic press. **b** Schematic experimental setup for MP method. **c** Uniform pressure actuator used in MP method. **d** Foil actuator shape and dimension used in vaporizing foil method. **e** Schematic experimental setup of direct VFA

the foil. For the urethane VFA, the width of the deformed region of the workpiece was between those of the active part of the foil actuator and the urethane pad.

Results and discussion

Depth of embossed groove

Figure 4a shows the relationship between the pressure and the measured depth of the groove on the deformed copper workpiece with static method. As expected, the depth of the groove increased with pressure. From the figure, one should notice that starting 600 MPa the copper workpiece was fully deformed. The size of the deformed copper was 25 mm × 15 mm, which was limited by the capacity of a press. Fig. 4b shows the embossed depth of the groove on copper sheet with high strain rate methods. The embossed depth increased with capacitor bank energy. With MP method, the highest depth of the formed groove on copper was 195 μm, 56 % of the full depth of groove on the die at capacitor bank energy of 6.4 kJ. The energy level was limited by the capacity of UPA. The deformed area has the dimension of 100 mm × 33 mm. Figure 4c shows the surface of copper deformed by the MP method from low to high magnification. The workpiece was not fully deformed. But the deformation was uniform over a larger area. With direct VFA method, full depth was achieved at capacitor bank energy of 3.2 kJ. The size of deformed copper was the same as that of the active area of the vaporizing foil, which is 100 mm × 15 mm in this study, much larger than the area studied in static forming. The deformation was found to be uniform. Although the groove depth could not increase any further, it can be expected that with higher energy levels, the strain rate would be higher. Figure 4d shows the cross section of one of the samples with full-depth groove. It was observed that the deformed copper had very good conformity with the die. With the urethane VFA method, the highest depth of the formed groove on copper was

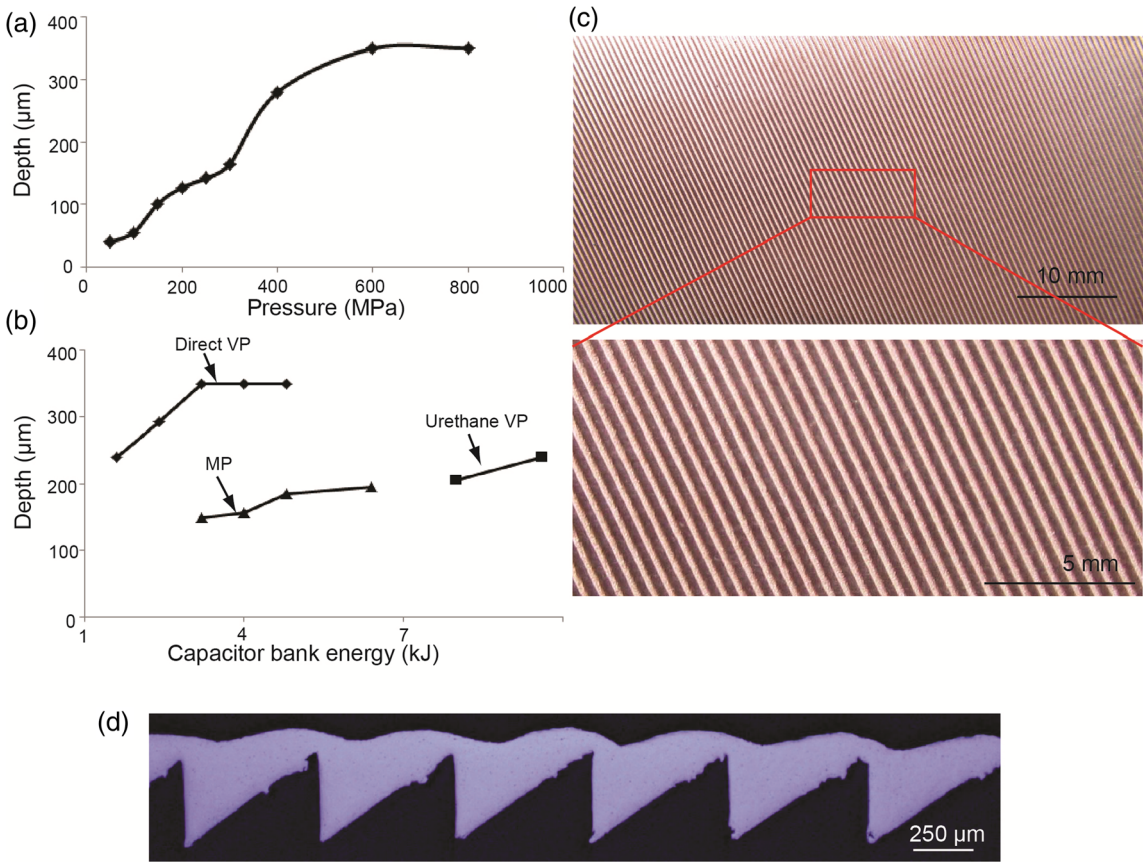

Fig. 4 **a** Depth of deformed workpieces VS. pressure in the static method. Full depth of the die was 350 μm. **b** Embossed depth of the deformed workpieces VS. capacitor bank energy with different high strain rate forming methods: MP, direct VFA, and urethane VFA. **c** Surface morphology of deformed copper workpiece from low magnification to high magnification with the MP method at capacitor bank energy of 6.4 kJ. **d** Cross section of fully deformed workpiece with the direct VFA method at 4.8 kJ capacitor bank energy

240 μm, which is 69 % of the full depth at an input energy level of 9.6 kJ. The size of deformed copper was the same as that of the urethane pad, which was 100 mm × 75 mm. However, the deformation was not uniform. The region directly above the vaporizing foil had the deepest embossed depth. When a shock wave travels within a medium, its energy decreases with travelled distance. Due to this reason, the central part of the workpiece was found to have the deepest embossed depth. A detailed accounting of these pressure distributions has been published elsewhere [21]. Therefore, with static and direct VFA methods, full depth can be achieved. The deformed area is 4 times larger with direct VFA method. To fabricate such area, 1 MN press will be required with static method. Furthermore, the area deformed with direct VFA can be increased by increase the dimension of the foil and capacitor bank energy.

With MP method, the velocity of the workpiece was measured, as shown in Fig. 5a. The impact velocity is the final workpiece velocity before its collision with die. Both the impact velocity and acceleration increased with capacitor bank energy. The relationship between the square of the workpiece velocity and the capacitor bank energy is shown in Fig. 5b. The slope of the fitting line is $2\eta/m$ (η is the energy efficiency and m is the mass of workpiece). It showed that the energy efficiency remained a constant with varying energy levels, which is 1.9 %. There were some deviations from the linear trend, which could be attributed to small experimental errors.

Micro-hardness

The average Vickers hardness of the as-received copper was 88 HV. Figure 6a shows the indent position on the deformed copper. Figure 6b shows the typical hardness distribution for one of the tested samples. From Fig. 6b, it can be deduced that the dramatic hardness change was found along the long edge of the groove. The bottom of the embossed groove was consistently found to be the location with highest hardness due to the severe plastic deformation. The average hardness of the tested area and the average hardness along the long edge were calculated for some samples, as shown in Fig. 7. The overall hardness increase was between 25 % and 41 %. The hardness increase along the long edge of the groove was between 43 and 53 %. It can be surmised that largest plastic strains were along the long edge of the formed groove.

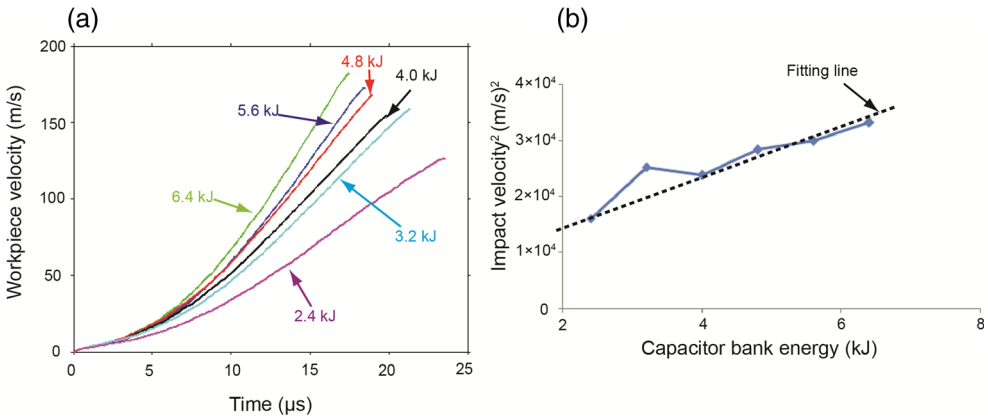

Fig. 5 **a** Flyert velocity at varied capacitor bank energy with the MP method. **b** Relationship between (Flyer velocity)^2 and capacitor bank energy in the MP method

For each forming method, hardness increased with embossed depth due to the increasing plastic deformation. For each sample, the long edge had higher hardness than the rest of tested area. Static and direct VFA methods had similar effect on the hardness increase before the sample fully deformed. Although direct VFA method is a high strain rate forming method, the temperature increase in the deformed sample due to its contact with hot plasma might counter the increase in hardness from the strain rate. After the sample fully deformed, with direct VFA method hardness can be increased by increasing the capacitor bank energy due to the increased strain rate and possibly increased redundant strain. At the same embossed depth of around 240 μm, the sample formed by direct VFA had lower hardness than the sample formed by the urethane VFA method, again, possibly attributed to heating due to the plasma generation. Therefore, strain rate significantly increased hardness as shown with the urethane VFA. At the same embossed depth of around 200 μm, the MP formed sample had a smaller hardness increase compared to the sample formed by urethane VFA, particularly on the regions away from contact. It may be that there is some effect of current and joule heating and the contacted surface helps harden the groove edges. It is most likely that the MP and urethane VFA have similar strain rate, which induced the similar microstructure along the long edge of the embossed groove.

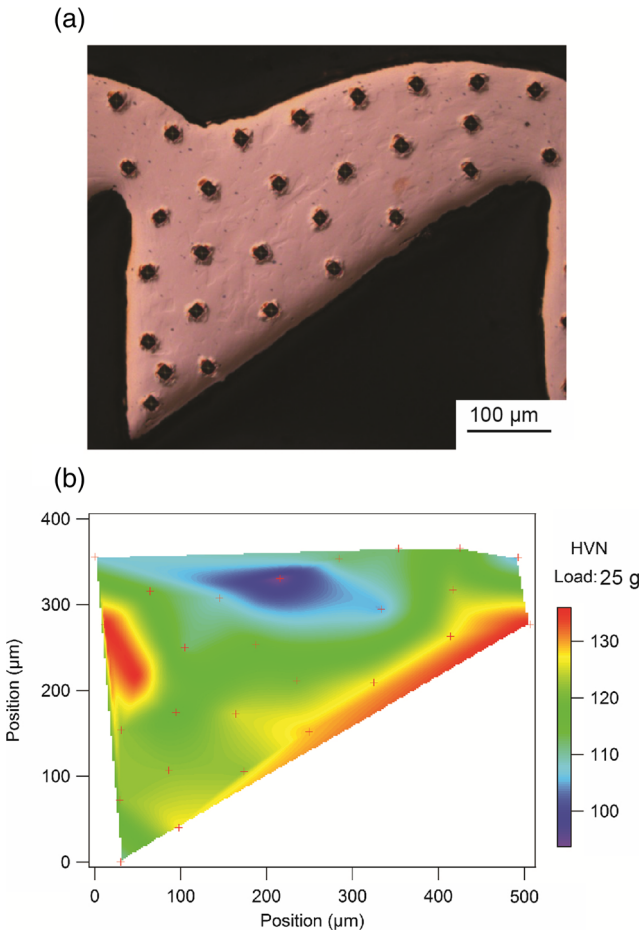

Fig. 6 **a** Micro hardness indent position on deformed copper workpiece. **b** Micro hardness map shows the hardness distribution on the deformed copper workpiece. This sample is formed with the direct VFA method at a capacitor bank energy of 4.8 kJ

The direct VFA method can significantly overdrive the process, producing much higher overall pressures than any of the other methods. This allows not only complete filling of the grooved geometry, but as the impulse energy increases there is a continued increase in hardness that can be attributed to increasing strain rate and possibly increased amounts of redundant strain.

Microstructure

The microstructure of the samples was studied with optical microscopy (OM), scanning electron microscopy (SEM) and transmission electron microscopy (TEM). The samples were polished down to a grit size of 0.05 μm. After that, they were etched by a solution of one third water, one third H_2O_2 (3 %) and one third NH_3OH. Figure 8 showed the microstructure of

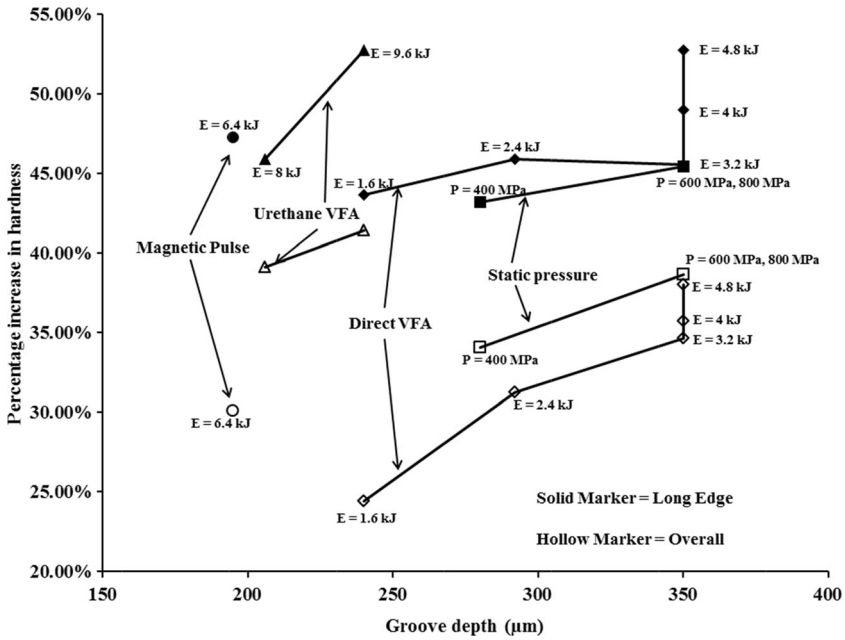

Fig. 7 Hardness increase for samples with different forming methods

two of the samples. One was formed with static forming method, and the other was formed by MP forming. Figure 8a showed the position where the microstructural samples were taken from. Figure 8c depicted the microstructure of MP formed copper at an energy level of 6.4 kJ. Unlike the static formed sample, a significant amount of twinning was observed in the MP formed sample as indicated by the regions within black dotted circles. High magnification SEM images were shown in Fig. 8e and f, which depicted the difference in microstructures. High strain rates enable the twinning to occur. The sample created by the static forming experienced more plastic deformation than the sample created by MP forming. However, the latter had a higher hardness value compared to the former one. It is quite evident that due to the difference in the strain rate, the deformation mechanisms were different during the mentioned processes. At low strain rates,

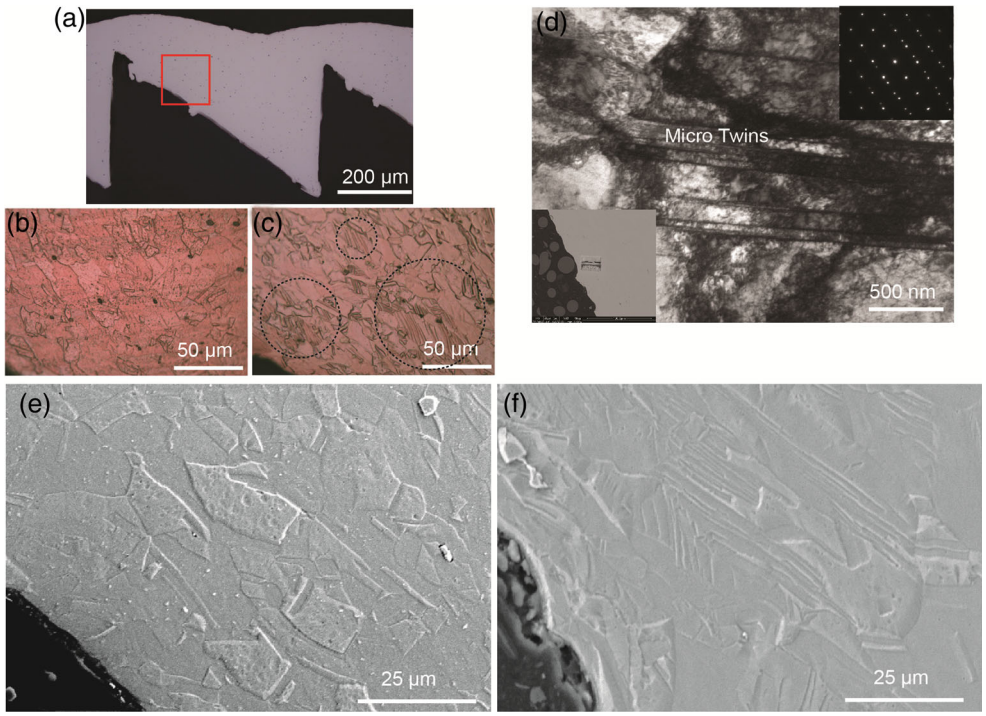

Fig. 8 **a** Cross section of deformed copper workpiece. The red square indicates the position where the (*b*) and (*c*) shows. **b** Microstructure of the sample with the static method. **c** Microstructure of the sample with the MP method. **d** Microstructure of the sample with MP method. Nano-twins and high density dislocation are observed. The upper left corner shows the diffraction pattern of nano-twins. Zone axis is [110] for the diffraction pattern. **e** SEM image shows microstructure of the sample with the static method. **f** SEM image shows microstructure of the sample with the MP method

dislocation sliding was the dominant deformation mechanism, whereas, at high strain rates occurring during MP forming, both dislocation sliding and twinning mechanisms were activated [16]. Figure 8d showed the TEM image and diffraction pattern of the sample with MP forming method. The lower left corner image showed that the TEM sample was taken at the location along the long edge of the embossed groove. Nano-twins and high dislocation density were observed. Therefore, MP method can be used to fabricate nanostructure materials. By comparing the hardness and deformed depth of the copper, urethane-vaporizing foil method can be another optional method to fabricate nanostructure materials. Direct VFA

Figure 9a showed the orientation imaging microscopy (OIM) image of sample with the direct VFA forming method at capacitor bank energy level of 4.8 kJ. It showed the grain elongation at the bottom of the groove. It also showed smaller grain size along the long edge due to the severe plastic deformation. The pole figure showed certain amount of texture appeared within the tested region. The deformation twins were not clearly shown in this figure. Figure 9 b and c showed the microstructure of the deformed copper with urethane VFA at 8.0 kJ and 9.6 kJ. The more severe plastic deformation resulted in a significant number of deformation twins along the long edge of the groove at 9.6 kJ. The black circle on Fig. 9b showed that significant twins appeared in the sample at 8.0 kJ. Much more amount of twining appeared in the sample with 9.6 kJ energy. The region where deformation twins appear was much larger than that in the sample

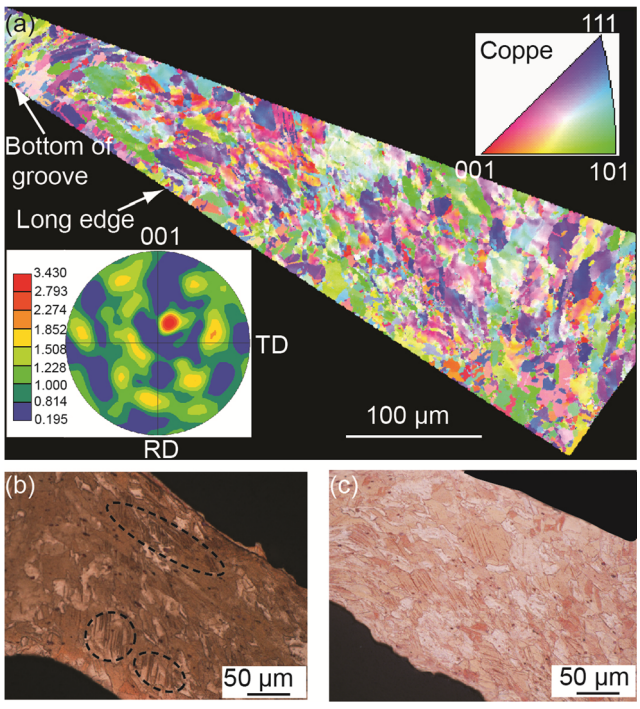

Fig. 9 **a** OIM image of a sample produced by the direct VFA method at the capacitor bank energy of 4.8 kJ. **b** Microstructure of the sample with the urethane VFA method at the capacitor bank energy of 8.0 kJ, and **c** 9.6 kJ

created at 8.0 kJ. Figure 9c depicted that the density of the deformation twins was higher along the long edge of the groove. It decreased with the distance away from the long edge. It can be seen that the size of the deformation twins was small along the long edge and became bigger away from the long edge in the sample thickness direction from Fig. 9c.

Conclusion

In this research, several methods that span a range of accessible pressures and strain rates were used to emboss fine features onto a copper sheet. These included: static forming, MP forming, direct VFA forming, and urethane VFA forming. These methods can both impart a complex geometry to the sheet and modify the microstructure and properties in important ways. The component with full depth of the die was achieved by static and the direct VFA method. With the MP method, 56 % of the full depth was achieved at the highest capacitor bank energy that the current UPA could withstand. With urethane VFA, the maximum depth of the groove was 69 % of the total depth with an input energy of 9.6 kJ. The main conclusions are as follows:

1) Comparing the embossed depth of the groove, direct VFA is a promising method for embossing. Full depth groove was achieved by the direct VFA. With the static forming method, to fabricate the embossed component with dimension of 100 mm × 15 mm, over 1 MN of press would be required, but equivalent dynamic pressures are easily achieved with the VFA method.
2) The hardness map showed that along the long edge of the embossed groove the hardness was higher than other regions. In general, higher strain rate processes (VFA and MP) gave higher hardness at the same groove depth (which is an indicator of plastic strain level). However, the direct VFA method had significantly lower hardness than the urethane VFA method where the plasma is shielded by urethane. This is likely because there is some heating by the plasma. Overdriving the driect method with higher energies also provided higher hardness.
3) In high strain rate deformed samples, significant twinning and high dislocation density were observed along the long edge. The amount of twining increased with increasing capacitor bank energy. The size of the twin was smaller along the long edge and became bigger away from it in the sample thickness direction. In low strain rate samples, there was no twinning observed.
4) TEM images showed nano-twins in the MP formed samples. The grain refinement and certain amount of texture were confirmed with OIM analysis. MP and urethane VFA methods are promising for the fabrication nanostructured materials.

Acknowledgment This work is funded by Alcoa Foundation. The authors thank members in the lab for the valuable discussion and help in the experiments, special thanks to Alexander Koenig for the help of static experimental work.

Compliance with ethical standards

Funding This study was funded by Alcoa Foundation.

Conflict of interest The authors declare that they have no conflict of interest.

References

1. Chan WL, Fu MW, Yang B (2011) Study of size effect in micro-extrusion process of pure copper. Mater Des 32(7):3772–3782. doi:10.1016/j.matdes.2011.03.045
2. Li XG, Sabir M (2005) Review of bipolar plates in PEM fuel cells: flow-field designs. Int J Hydrog Energy 30(4):359–371. doi:10.1016/j.ijhydene.2004.09.019
3. Mai JM, Peng LF, Lai XM, Lin ZQ (2013) Electrical-assisted embossing process for fabrication of micro-channels on 316 L stainless steel plate. J Mater Process Technol 213(2):314–321. doi:10.1016/j.jmatprotec.2012.09.013
4. Vollertsen F, Niehoff HS, Hu Z (2006) State of the art in micro forming. Int J Mach Tools Manuf 46(11):1172–1179. doi:10.1016/j.ijmachtools.2006.01.033
5. Mahabunphachai S, Koc M (2008) Investigation of size effects on material behavior of thin sheet metals using hydraulic bulge testing at micro/meso-scales. Int J Mach Tools Manuf 48(9):1014–1029. doi:10.1016/j.ijmachtools.2008.01.006
6. Gau JT, Principe C, Wang JW (2007) An experimental study on size effects on flow stress and formability of aluminm and brass for microforming. J Mater Process Technol 184(1–3):42–46. doi:10.1016/j.jmatprotec.2006.11.003
7. Conrad H (2000) Electroplasticity in metals and ceramics. Mat Sci Eng a-Struc Mat Prop Mic Proc 287(2):276–287. doi:10.1016/s0921-5093(00)00786-3
8. Troitskii OA, Likhtman VI (1963) Anisotropy of the effect of electron-beam and α-irradiation on the deformation process of zinc single crystals in the brittle state. Akademii Nauk SSSR 148(2):332–334
9. Troitskii OA (1977) Effect of the electron state of a metal on its mechanical properties and the phenomenon of electroplasticity. J Sandw Struct Mater 9:35–45
10. Daehn GS (2006) High velocity metal forming. ASM handbook: Metalworking-sheet forming 14B:405–418
11. Iriondo E, Gutierrez MA, Gonzalez B, Alcaraz JL, Daehn GS (2011) Electromagnetic impulse calibration of high strength sheet metal structures. J Mater Process Technol 211(5):909–915. doi:10.1016/j.jmatprotec.2010.05.013
12. Meyers MA, Andrade UR, Chokshi AH (1995) The effect of grain size on the high strain, high strain rate behavior of copper. Metal Mat Trans a-Physical Met Mat Scie 26(11):2881–2893. doi:10.1007/bf02669646
13. Meyers MA, Gregori F, Kad BK, Schneider MS, Kalantar DH, Remington BA, Ravichandran G, Boehly T, Wark JS (2003) Laser-induced shock compression of monocrystalline copper: characterization and analysis. Acta Mater 51(5):1211–1228. doi:10.1016/s1359-6454(02)00420-2
14. Liao XZ, Zhao YH, Srinivasan SG, Zhu YT, Valiev RZ, Gunderov DV (2004) Deformation twinning in nanocrystalline copper at room temperature and low strain rate. Appl Phys Lett 84(4):592–594. doi:10.1063/1.1644051
15. Rohatgi A, Vecchio KS (2002) The variation of dislocation density as a function of the stacking fault energy in shock-deformed FCC materials. Mat Sci Eng a-Struc Mat Prop Mic Proc 328(1–2):256–266. doi:10.1016/s0921-5093(01)01702-6
16. Li YS, Tao NR, Lu K (2008) Microstructural evolution and nanostructure formation in copper during dynamic plastic deformation at cryogenic temperatures. Acta Mater 56(2):230–241. doi:10.1016/j.actamat.2007.09.020
17. Chan HL, Ruan HH, Chen AY, Lu J (2010) Optimization of the strain rate to achieve exceptional mechanical properties of 304 stainless steel using high speed ultrasonic surface mechanical attrition treatment. Acta Mater 58(15):5086–5096. doi:10.1016/j.actamat.2010.05.044
18. Li YS, Zhang Y, Tao NR, Lu K (2009) Effect of the Zener-Hollomon parameter on the microstructures and mechanical properties of Cu subjected to plastic deformation. Acta Mater 57(3):761–772. doi:10.1016/j.actamat.2008.10.021
19. Konkova T, Mironov S, Korznikov A, Semiatin SL (2010) Microstructural response of pure copper to cryogenic rolling. Acta Mater 58(16):5262–5273. doi:10.1016/j.actamat.2010.05.056
20. Kamal M, Daehn GS (2007) A uniform pressure electromagnetic actuator for forming flat sheets. J Manuf Scie Eng Trans Asme 129(2):369–379. doi:10.1115/1.2515481
21. Vivek A, Brune RC, Hansen SR, Daehn GS (2014) Vaporizing foil actuator used for impulse forming and embossing of titanium and aluminum alloys. J Mater Process Technol 214(4):865–875. doi:10.1016/j.jmatprotec.2013.12.003
22. Vivek A (2012) Rapid vaporization of thin conductors used for impulse metalworking. The Ohio State University Thesis
23. Vivek A, Taber GA, Johnson JR, Woodward ST, Daehn GS (2013) Electrically driven plasma via vaporization of metallic conductors: a tool for impulse metal working. J Mater Process Technol 213(8):1311–1326. doi:10.1016/j.jmatprotec.2013.02.010
24. Johnson JR, Taber G, Vivek A, Zhang Y, Golowin S, Banik K, Fenton GK, Daehn GS (2009) Coupling experiment and simulation in electromagnetic forming using photon Doppler Velocimetry. J Iron Steel Res Int 80(5):359–365. doi:10.2374/sri08sp160